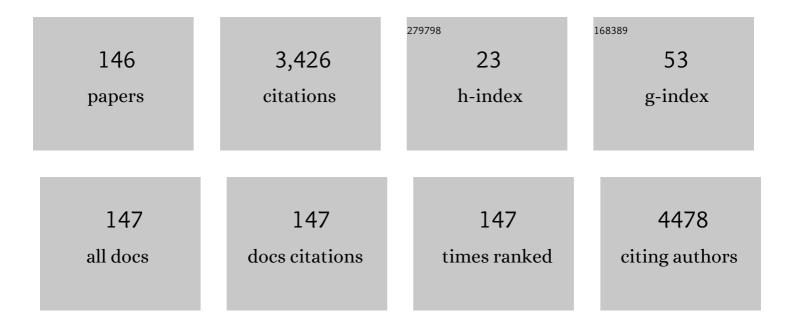
List of Publications by Year in descending order

Source: https://exaly.com/author-pdf/3162599/publications.pdf Version: 2024-02-01



#	Article	IF	CITATIONS
1	A review of 3D vessel lumen segmentation techniques: Models, features and extraction schemes. Medical Image Analysis, 2009, 13, 819-845.	11.6	775
2	Evidence for potentials and limitations of brain plasticity using an atlas of functional resectability of WHO grade II gliomas: Towards a "minimal common brain― NeuroImage, 2011, 56, 992-1000.	4.2	325
3	Association Between Long-term Exposure to Ambient Air Pollution and Change in Quantitatively Assessed Emphysema and Lung Function. JAMA - Journal of the American Medical Association, 2019, 322, 546.	7.4	236
4	A State-of-the-Art Review on Segmentation Algorithms in Intravascular Ultrasound (IVUS) Images. IEEE Transactions on Information Technology in Biomedicine, 2012, 16, 823-834.	3.2	114
5	LV volume quantification via spatiotemporal analysis of real-time 3-D echocardiography. IEEE Transactions on Medical Imaging, 2001, 20, 457-469.	8.9	106
6	Segmentation of real-time three-dimensional ultrasound for quantification of ventricular function: A clinical study on right and left ventricles. Ultrasound in Medicine and Biology, 2005, 31, 1143-1158.	1.5	96
7	Glioma Dynamics and Computational Models: A Review of Segmentation, Registration, and In Silico Growth Algorithms and their Clinical Applications. Current Medical Imaging, 2007, 3, 262-276.	0.8	93
8	Compressed sensing with off-axis frequency-shifting holography. Optics Letters, 2010, 35, 871.	3.3	81
9	Discriminative Localization in CNNs for Weakly-Supervised Segmentation of Pulmonary Nodules. Lecture Notes in Computer Science, 2017, 10435, 568-576.	1.3	78
10	Simultaneous left atrium anatomy and scar segmentations via deep learning in multiview information with attention. Future Generation Computer Systems, 2020, 107, 215-228.	7.5	73
11	An Unbiased Risk Estimator for Image Denoising in the Presence of Mixed Poisson–Gaussian Noise. IEEE Transactions on Image Processing, 2014, 23, 1255-1268.	9.8	70
12	Denoising of Microscopy Images: A Review of the State-of-the-Art, and a New Sparsity-Based Method. IEEE Transactions on Image Processing, 2018, 27, 3842-3856.	9.8	63
13	Off-axis compressed holographic microscopy in low-light conditions. Optics Letters, 2011, 36, 79.	3.3	50
14	Region-Based Endocardium Tracking on Real-Time Three-Dimensional Ultrasound. Ultrasound in Medicine and Biology, 2009, 35, 256-265.	1.5	47
15	Real-time segmentation by Active Geometric Functions. Computer Methods and Programs in Biomedicine, 2010, 98, 223-230.	4.7	42
16	Dynamic osmotic loading of chondrocytes using a novel microfluidic device. Journal of Biomechanics, 2005, 38, 1273-1281.	2.1	38
17	Automatic Segmentation of Antenatal 3-D Ultrasound Images. IEEE Transactions on Biomedical Engineering, 2013, 60, 1388-1400.	4.2	36
18	Whole-body pregnant woman modeling by digital geometry processing with detailed uterofetal unit based on medical images. IEEE Transactions on Biomedical Engineering, 2010, 57, 2346-2358.	4.2	35

#	Article	IF	CITATIONS
19	Imaging and 3D morphological analysis of collagen fibrils. Journal of Microscopy, 2012, 247, 161-175.	1.8	33
20	Adaptive particle filtering for coronary artery segmentation from 3D CT angiograms. Computer Vision and Image Understanding, 2016, 151, 29-46.	4.7	28
21	A Longitudinal Cohort Study of Aspirin Use and Progression of Emphysema-like Lung Characteristics on CT Imaging. Chest, 2018, 154, 41-50.	0.8	28
22	Segmentation of embryonic and fetal 3D ultrasound images based on pixel intensity distributions and shape priors. Medical Image Analysis, 2015, 24, 255-268.	11.6	26
23	State of the Art of Level Set Methods in Segmentation and Registration of Medical Imaging Modalities. , 2005, , 47-101.		25
24	Medial-based Bayesian tracking for vascular segmentation: Application to coronary arteries in 3D CT angiography. , 2008, , .		24
25	Automatic segmentation of head structures on fetal MRI. , 2009, , .		24
26	Adaptive Quantification and Longitudinal Analysis of Pulmonary Emphysema With a Hidden Markov Measure Field Model. IEEE Transactions on Medical Imaging, 2014, 33, 1527-1540.	8.9	23
27	Quasi-automatic 3D reconstruction of the full spine from low-dose biplanar X-rays based on statistical inferences and image analysis. European Spine Journal, 2019, 28, 658-664.	2.2	23
28	Multiview Two-Task Recursive Attention Model for Left Atrium and Atrial Scars Segmentation. Lecture Notes in Computer Science, 2018, , 455-463.	1.3	23
29	Unravelling machine learning: insights in respiratory medicine. European Respiratory Journal, 2019, 54, 1901216.	6.7	22
30	Brain MRI Segmentation with Multiphase Minimal Partitioning: A Comparative Study. International Journal of Biomedical Imaging, 2007, 2007, 1-15.	3.9	21
31	VALIDATION OF OPTICAL-FLOW FOR QUANTIFICATION OF MYOCARDIAL DEFORMATIONS ON SIMULATED RT3D ULTRASOUND. , 2007, , .		20
32	Differential MRI analysis for quantification of low grade glioma growth. Medical Image Analysis, 2012, 16, 114-126.	11.6	19
33	Birthweight and patterns of postnatal weight gain in very and extremely preterm babies in England and Wales, 2008–19: a cohort study. The Lancet Child and Adolescent Health, 2021, 5, 719-728.	5.6	19
34	Bayesian Maximal Paths for Coronary Artery Segmentation from 3D CT Angiograms. Lecture Notes in Computer Science, 2009, 12, 222-229.	1.3	19
35	Design and study of flux-based features for 3D vascular tracking. , 2009, , .		18
36	A New Fuzzy Connectivity Measure for Fuzzy Sets. Journal of Mathematical Imaging and Vision, 2009, 34, 107-136.	1.3	18

#	Article	lF	CITATIONS
37	Joint variational segmentation of CT-PET data for tumoral lesions. , 2010, , .		17
38	Review of Myocardial Motion Estimation Methods from Optical Flow Tracking on Ultrasound Data. , 2006, 2006, 1537-40.		16
39	Surface Function Actives. Journal of Visual Communication and Image Representation, 2009, 20, 478-490.	2.8	16
40	Changes in neonatal admissions, care processes and outcomes in England and Wales during the COVID-19 pandemic: a whole population cohort study. BMJ Open, 2021, 11, e054410.	1.9	16
41	Assessment of visual quality and spatial accuracy of fast anisotropic diffusion and scan conversion algorithms for real-time three-dimensional spherical ultrasound. , 2004, , .		15
42	Tracking of LV Endocardial Surface on Real-Time Three-Dimensional Ultrasound with Optical Flow. Lecture Notes in Computer Science, 2005, , 434-445.	1.3	15
43	Dynamic Cardiac Information From Optical Flow Using Four Dimensional Ultrasound. , 2005, 2005, 4465-8.		15
44	Comparison of reconstruction algorithms in compressed sensing applied to biological imaging. , 2011, , .		15
45	Video reconstruction using compressed sensing measurements and 3d total variation regularization for bio-imaging applications. , 2012, , .		15
46	Maximum Likelihood Estimation of Shear Wave Speed in Transient Elastography. IEEE Transactions on Medical Imaging, 2014, 33, 1338-1349.	8.9	15
47	Evaluation of optical flow algorithms for tracking endocardial surfaces on three-dimensional ultrasound data. , 2005, , .		14
48	Effects of slice thickness and head rotation when measuring glioma sizes on MRI: in support of volume segmentation versus two largest diameters methods. Journal of Neuro-Oncology, 2013, 112, 165-172.	2.9	14
49	Suggestive Annotation of Brain Tumour Images with Gradient-Guided Sampling. Lecture Notes in Computer Science, 2020, , 156-165.	1.3	14
50	Vertebral rotation estimation from frontal X-rays using a quasi-automated pedicle detection method. European Spine Journal, 2019, 28, 3026-3034.	2.2	13
51	Unsupervised Discovery of Spatially-Informed Lung Texture Patterns for Pulmonary Emphysema: The MESA COPD Study. Lecture Notes in Computer Science, 2017, 10433, 116-124.	1.3	13
52	Multiview Sequential Learning and Dilated Residual Learning for a Fully Automatic Delineation of the Left Atrium and Pulmonary Veins from Late Gadolinium-Enhanced Cardiac MRI Images. , 2018, 2018, 1123-1127.		12
53	Automatic Brain Tumour Segmentation and Biophysics-Guided Survival Prediction. Lecture Notes in Computer Science, 2020, , 61-72.	1.3	12
54	Quantitative validation of optical flow based myocardial strain measures using sonomicrometry. , 2009, 2009, 454-457.		11

#	Article	IF	CITATIONS
55	Hybrid 3D pregnant woman and fetus modeling from medical imaging for dosimetry studies. International Journal of Computer Assisted Radiology and Surgery, 2010, 5, 49-56.	2.8	11
56	Automatic detection of luminal borders in IVUS images by magnitude-phase histograms of complex brushlet coefficients. , 2010, 2010, 3073-6.		11
57	BM3D-based ultrasound image denoising via brushlet thresholding. , 2015, , .		11
58	Coronary Occlusion Detection with 4D Optical Flow Based Strain Estimation on 4D Ultrasound. Lecture Notes in Computer Science, 2009, , 211-219.	1.3	11
59	Quantifying Brain [ <sup>18</sup> F]FDG Uptake Noninvasively by Combining Medical Health Records and Dynamic PET Imaging Data. IEEE Journal of Biomedical and Health Informatics, 2019, 23, 2576-2582.	6.3	10
60	Identification of variation in nutritional practice in neonatal units in England and association with clinical outcomes using agnostic machine learning. Scientific Reports, 2021, 11, 7178.	3.3	10
61	Explaining Radiological Emphysema Subtypes with Unsupervised Texture Prototypes: MESA COPD Study. Lecture Notes in Computer Science, 2017, 2017, 69-80.	1.3	10
62	Comparison study of clinical 3D MRI brain segmentation evaluation. , 2004, 2004, 1671-4.		9
63	Segmentation and quantitative evaluation of brain MRI data with a multiphase 3D implicit deformable model. , 2004, 5370, 526.		9
64	Compressed sensing in biological microscopy. , 2009, , .		9
65	Alzheimer's disease diagnosis based on anatomically stratified texture analysis of the hippocampus in structural MRI. , 2018, , .		9
66	Vertebral corners detection on sagittal X-rays based on shape modelling, random forest classifiers and dedicated visual features. Computer Methods in Biomechanics and Biomedical Engineering: Imaging and Visualization, 2019, 7, 132-144.	1.9	9
67	Segmentation of fetal 3D ultrasound based on statistical prior and deformable model. , 2008, , .		8
68	A compressed sensing approach for biological microscopic image processing. , 2009, , .		8
69	Toward Noninvasive Quantification of Brain Radioligand Binding by Combining Electronic Health Records and Dynamic PET Imaging Data. IEEE Journal of Biomedical and Health Informatics, 2015, 19, 1271-1282.	6.3	8
70	Texton and sparse representation based texture classification of lung parenchyma in CT images. , 2016, 2016, 1276-1279.		8
71	Generative method to discover emphysema subtypes with unsupervised learning using lung macroscopic patterns (LMPS): The MESA COPD study. , 2017, 2017, 375-378.		8
72	Characterizing Alzheimer's Disease With Image and Genetic Biomarkers Using Supervised Topic Models. IEEE Journal of Biomedical and Health Informatics, 2020, 24, 1180-1187.	6.3	8

#	Article	IF	CITATIONS
73	Multi-phase Three-Dimensional Level Set Segmentation of Brain MRI. Lecture Notes in Computer Science, 2004, , 318-326.	1.3	8
74	Combining Radiometric and Spatial Structural Information in a New Metric for Minimal Surface Segmentation. Lecture Notes in Computer Science, 2007, 20, 283-295.	1.3	8
75	Optimized Region Finding and Edge Detection of Knee Cartilage Surfaces from Magnetic Resonance Images. Annals of Biomedical Engineering, 2003, 31, 336-345.	2.5	7
76	Tracking Endocardium Using Optical Flow along Iso-Value Curve. , 2006, 2006, 707-10.		7
77	Superresolution spatial compounding techniques with application to 3D breast ultrasound imaging. , 2006, , .		7
78	Denoising in fluorescence microscopy using compressed sensing with multiple reconstructions and non-local merging. , 2010, 2010, 3394-7.		7
79	Compressed sensing-enabled phase-sensitive swept-source optical coherence tomography. Optics Express, 2019, 27, 855.	3.4	7
80	Transfer Learning from Partial Annotations for Whole Brain Segmentation. Lecture Notes in Computer Science, 2019, , 199-206.	1.3	7
81	Emphysema Quantification on Cardiac CT Scans Using Hidden Markov Measure Field Model: The MESA Lung Study. Lecture Notes in Computer Science, 2016, 9901, 624-631.	1.3	7
82	Segmentation of fetal envelope from 3D ultrasound images based on pixel intensity statistical distribution and shape priors. , 2013, , .		6
83	Sparse sampling and unsupervised learning of lung texture patterns in pulmonary emphysema: MESA COPD study. , 2015, , .		6
84	Image denoising by multiple compressed sensing reconstructions. , 2015, , .		6
85	Lumbar spine posterior corner detection in X-rays using Haar-based features. , 2016, , .		6
86	Using Artificial Intelligence in Fungal Lung Disease: CPA CT Imaging as an Example. Mycopathologia, 2021, 186, 733-737.	3.1	6
87	Novel Subtypes of Pulmonary Emphysema Based on Spatially-Informed Lung Texture Learning: The Multi-Ethnic Study of Atherosclerosis (MESA) COPD Study. IEEE Transactions on Medical Imaging, 2021, 40, 3652-3662.	8.9	6
88	Lumen Border Detection of Intravascular Ultrasound via Denoising of Directional Wavelet Representations. Lecture Notes in Computer Science, 2009, , 104-113.	1.3	6
89	Utero-Fetal Unit and Pregnant Woman Modeling Using a Computer Graphics Approach for Dosimetry Studies. Lecture Notes in Computer Science, 2009, 12, 1025-1032.	1.3	6
90	ADAPTIVE SEGMENTATION OF INTERNAL BRAIN STRUCTURES IN PATHOLOGICAL MR IMAGES DEPENDING ON TUMOR TYPES. , 2007, , .		5

#	Article	IF	CITATIONS
91	Integrated multimedia electronic patient record and graph-based image information for cerebral tumors. Computers in Biology and Medicine, 2008, 38, 425-437.	7.0	5
92	Numerical evaluation of sampling bounds for near-optimal reconstruction in compressed sensing. , 2011, , .		5
93	Reducing data acquisition for fast Structured Illumination Microscopy using Compressed Sensing. , 2017, , .		5
94	Variational segmentation framework in prolate spheroidal coordinates for 3D real-time echocardiography. , 2006, , .		4
95	Segmentation of the fetal envelope on ante-natal MRI. , 2010, , .		4
96	Measurement of the Skin-Liver Capsule Distance on Ultrasound RF Data for 1D Transient Elastography. Lecture Notes in Computer Science, 2010, 13, 34-41.	1.3	4
97	Brushlet segmentation for automatic detection of lumen borders in IVUS images: A comparison study. , 2012, , .		4
98	Locally weighted total variation denoising for ringing artifact suppression in pet reconstruction using PSF modeling. , 2013, 2013, 1252-1255.		4
99	Robust quantification of pulmonary emphysema with a Hidden Markov Measure Field model. , 2013, , .		4
100	Unsupervised Domain Adaption With Adversarial Learning (UDAA) for Emphysema Subtyping on Cardiac CT Scans: The Mesa Study. , 2019, , .		4
101	Encoding Human Cortex Using Spherical CNNs - A Study on Alzheimer's Disease Classification. , 2020, , .		4
102	An incremental and optimized learning method for the automatic classification of protein crystal images. , 2006, Suppl, 6526-9.		3
103	Compressed sensing applications for biological microscopy. , 2010, , .		3
104	Vessel geometry modeling and segmentation using convolution surfaces and an implicit medial axis. , 2011, , .		3
105	Accurate and robust shape descriptors for the identification of RIB cage structures in CT-images with Random Forests. , 2013, , .		3
106	Sparsity-based simplification of spectral-domain optical coherence tomography images of cardiac samples. , 2016, , .		3
107	Self-training for Brain Tumour Segmentation with Uncertainty Estimation and Biophysics-Guided Survival Prediction. Lecture Notes in Computer Science, 2021, , 514-523.	1.3	3
108	Heterogeneity Measurement of Cardiac Tissues Leveraging Uncertainty Information from Image Segmentation. Lecture Notes in Computer Science, 2020, 12261, 782-791.	1.3	3

#	Article	IF	CITATIONS
109	Specificities of Physiological Signals and Medical Images. , 0, , 43-76.		2
110	Compressed Sensing in microscopy with random projections in the Fourier domain. , 2009, , .		2
111	Classification of blood regions in IVUS images using three dimensional brushlet expansions. , 2009, 2009, 471-4.		2
112	Contrast mapping and statistical testing for low-grade glioma growth quantification on brain MRI. , 2010, , .		2
113	Parameterization of real-time 3D speckle tracking framework for cardiac strain assessment. , 2011, 2011, 2654-7.		2
114	Non-invasive quantification of brain [ <sup>18</sup> F]-FDG uptake by combining medical health records and dynamic PET imaging data. , 2015, 2015, 2243-6.		2
115	Image denoising by adaptive Compressed Sensing reconstructions and fusions. Proceedings of SPIE, 2015, , .	0.8	2
116	Co-Seg: An Image Segmentation Framework Against Label Corruption. , 2021, , .		2
117	Enhanced-Quality Gan (EQ-GAN) on Lung CT Scans: Toward Truth and Potential Hallucinations. , 2021, ,		2
118	Evaluation of in vivo Liver Tissue Characterization with Spectral RF Analysis versus Elasticity. Lecture Notes in Computer Science, 2011, 14, 387-395.	1.3	2
119	A sparsity-based simplification method for segmentation of spectral-domain optical coherence tomography images. , 2017, , .		2
120	Automated Spinal Midline Delineation on Biplanar X-Rays Using Mask R-CNN. Lecture Notes in Computational Vision and Biomechanics, 2019, , 307-316.	0.5	2
121	Recognition of micro-array protein crystals images using multi-scale representations. , 2005, , .		1
122	Real-time segmentation of 4D ultrasound by Active Geometric Functions. , 2008, , .		1
123	Fibroscan $\hat{A}^{\circledast}$ practice improvement with a real-time assistance ultrasound tool: a premiminary study. , 2009, , .		1
124	Compressed sensing for digital holographic microscopy. , 2010, , .		1
125	Numerical evaluation of subsampling effects on image reconstruction in compressed sensing microscopy. , 2011, , .		1
126	Impact of temporal resolution on LV myocardial regional strain assessment with real-time 3D ultrasound. , 2012, 2012, 4075-8.		1

#	Article	IF	CITATIONS
127	Conciliating syntactic and semantic constraints for multi-phase and multi-channel region segmentation. Computer Vision and Image Understanding, 2013, 117, 819-826.	4.7	1
128	Phase retrieval with sparsity priors and application to microscopy video reconstruction. , 2013, , .		1
129	Equating emphysema scores and segmentations across CT reconstructions: A comparison study. , 2015, , .		1
130	Machine-Learning on Liver Ultrasound to Stratify Multiple Diseases via Blood-Vessels and Perfusion Characteristics. , 2020, , .		1
131	Segmentation and Uncertainty Measures of Cardiac Substrates within Optical Coherence Tomography Images via Convolutional Neural Networks. , 2020, , .		1
132	Applications of Multiscale Overcomplete Wavelet-Based Representations in Intravascular Ultrasound (IVUS) Images. , 2012, , 313-336.		1
133	Novel Application of Microfluidic Channels in Studying Cell Migration and Reorientation in Response to Direct Current Electric Fields. , 2002, , 243.		0
134	Physics-Based Modeling of the Pregnant Woman. Lecture Notes in Computer Science, 2010, , 71-81.	1.3	0
135	Implicit medial representation for vessel segmentation. Proceedings of SPIE, 2011, , .	0.8	0
136	Segmentation-free and multiscale-free extraction of medial information using Gradient Vector Flow — Application to vascular structures. , 2012, , .		0
137	Biological video reconstruction using linear or non-linear Fourier measurements. Proceedings of SPIE, 2013, , .	0.8	Ο
138	Toward diagnostic criteria for left ventricular systolic dysfunction from myocardial deformation. , 2014, , .		0
139	Locally weighted total variation denoising for PSF modeling artifact suppression in PET reconstruction. , 2014, , .		0
140	Guest Editorial IEEE EMBC 2015. IEEE Journal of Biomedical and Health Informatics, 2016, 20, 1215-1215.	6.3	0
141	Automatic Segmentation and Identification of Spinous Processes on Sagittal X-Rays Based on Random Forest Classification and Dedicated Contextual Features. , 2019, , .		0
142	Enhanced Generative Model for Unsupervised Discovery of Spatially-Informed Macroscopic Emphysema: The Mesa Copd Study. , 2019, , .		0
143	3d Pathological Signs Detection And Scoring On CPA CT Lung Scans. , 2021, , .		0
144	Unsupervised Clustering Of Airway Tree Structures On High-Resolution CT: The Mesa Lung Study. , 2021, , .		0

#	Article	IF	CITATIONS
145	Tracking Endocardium Using Optical Flow along Iso-Value Curve. , 2008, , 337-360.		Ο
146	Post-natal growth of very preterm neonates – Authors' reply. The Lancet Child and Adolescent Health, 2022, 6, e11.	5.6	0